

# Redox Behavior of Vanadium Oxide Nanotubes As Studied by X-ray Photoelectron Spectroscopy and Soft X-ray Absorption Spectroscopy

Sara Nordlinder,<sup>\*,†</sup> Andreas Augustsson,<sup>‡</sup> Thorsten Schmitt,<sup>‡</sup> Jinghua Guo,<sup>§</sup> Laurent C. Duda,<sup>‡</sup> Joseph Nordgren,<sup>‡</sup> Torbjörn Gustafsson,<sup>†</sup> and Kristina Edström<sup>†</sup>

Department of Materials Chemistry, Uppsala University, Box 538, SE-751 21 Uppsala, Sweden, Department of Physics, Uppsala University, Box 530, SE-751 21 Uppsala, Sweden, and Advanced Light Source, Lawrence Berkeley National Laboratory, Berkeley, California 94720

Received January 8, 2003. Revised Manuscript Received April 11, 2003

Ex situ soft X-ray absorption spectroscopy (SXAS) and X-ray photoelectron spectroscopy (XPS) were used to study the redox behavior of sodium-containing vanadium oxide (Na-VO<sub>x</sub>) nanotubes in a rechargeable Li battery context. This nanotubular material consists of scroll-like layers of vanadium oxide separated by structure-directing agents, in this case Na<sup>+</sup> ions. As lithium ions are inserted into the Na-VO<sub>x</sub> nanotubes, the V 2p peak weight shifts toward lower energies. This effect can be seen in both the SXAS and XPS results. Average oxidation states could be obtained from the XPS results, and these agree well with those estimated from electrochemical measurements. At potentials below 2.0 V, there is a coexistence of V(V), V(IV), and V(III), which suggests that some of the vanadium is inaccessible to reduction during the first cycles.

## Introduction

Vanadium oxide nanotubes recently proved to be a functioning cathode material for rechargeable Li batteries.<sup>1–3</sup> This investigation addresses the lithium intercalation process and the resulting change of the vanadium oxidation state.

Since the early 1990s, an increasing number of reports have been published on transition metal oxide nanotubes, including ZnO,<sup>4</sup> MoO<sub>3</sub>,<sup>5</sup> TiO<sub>2</sub>,<sup>6,7</sup> ZrO<sub>2</sub>,<sup>8</sup> and Co<sub>3</sub>O<sub>4</sub>.<sup>9</sup> Vanadium oxide (VO<sub>x</sub>) nanotubes, consisting of scroll-like layers of vanadium oxide, were first reported in 1998.<sup>10</sup> These redox-active nanotubes are prepared by a templating approach in which primary alkylamines

act as structure-directing molecules.<sup>11,12</sup> An initial sol-gel reaction of vanadium(V) alkoxide precursors together with alkylamines, followed by hydrothermal treatment, produces nanotubes consisting of multiple layers of vanadium oxide separated by the templating molecules. Normally, the tubes are 0.5–10 μm long and have open ends with outer diameters of 15–100 nm.

The embedded amine can readily be exchanged for other amines or for alkali, alkaline earth, or 3d transition metal ions, without destroying the tubular structure.<sup>13</sup> The ratio of guest charges (amines or cations) to vanadium atoms is always close to 0.27,<sup>3,13</sup> indicating that there are a fixed number of binding sites for the guest moieties. However, if the embedded guests are completely removed, by heating, for example, the structure collapses.

Many vanadium oxides have been investigated as alternative cathode materials for rechargeable Li batteries. Some of the more studied systems are V<sub>2</sub>O<sub>5</sub>,<sup>14</sup> V<sub>6</sub>O<sub>13</sub>,<sup>15</sup> and Li<sub>1+x</sub>V<sub>3</sub>O<sub>8</sub>.<sup>16</sup> Vanadium oxide nanotubes can reversibly insert and extract Li<sup>+</sup> ions with capacities comparable to those of other cathode materials.<sup>1–3</sup> We

\* To whom correspondence should be addressed. Telephone: +46 18 4713701. Fax: +46 18 513548. E-mail: sara.nordlinder@mkem.uu.se.

<sup>†</sup> Department of Materials Chemistry, Uppsala University.

<sup>‡</sup> Department of Physics, Uppsala University.

<sup>§</sup> Lawrence Berkeley National Laboratory.

(1) Nordlinder, S.; Edström, K.; Gustafsson, T. *Electrochem. Solid State Lett.* **2001**, *4*, A129.

(2) Doble, A.; Ngala, K.; Shoufeng, T.; Zavalij, P. Y.; Whittingham, M. S. *Chem. Mater.* **2001**, *13*, 4382.

(3) Nordlinder, S.; Lindgren, J.; Gustafsson, T.; Edström, K. *J. Electrochem. Soc.* **2003**, *150*, E280.

(4) Zhang, J.; Sun, L.; Liao, C.; Yan, C. *Chem. Commun.* **2002**, *3*, 262.

(5) Satishkumar, B. C.; Govindaraj, A.; Vogl, E. M.; Basumallick, L.; Rao, C. N. R. *J. Mater. Res.* **1997**, *12*, 604.

(6) Zhang, M.; Bando, Y.; Wada, K. *J. Mater. Sci. Lett.* **2001**, *20*, 167.

(7) Ksuga, T.; Hiramatsu, M.; Hoson, A.; Sekino, T.; Niihara, K. *Langmuir* **1998**, *14*, 3160.

(8) Rao, C. N. R.; Satishkumar, B. C.; Govindaraj, A. *Chem. Commun.* **1997**, *16*, 1581.

(9) Shi, X.; Raymond, S. H.; Sanedrin, J.; Galvez, C.; Ho, D. G.; Hernandez, B.; Zhou, F.; Selke, M. *Nano Lett.* **2002**, *2*, 289.

(10) Spahr, M. E.; Bitterli, P.; Nesper, R.; Müller, M.; Krumeich, F.; Nissen, H. U. *Angew. Chem., Int. Ed.* **1998**, *37*, 1263.

(11) Muhr, H.-J.; Krumeich, F.; Schönholzer, U. P.; Bieri, F.; Niederberger, M.; Gauckler, L. J.; Nesper, R. *Adv. Mater.* **2000**, *12*, 231.

(12) Krumeich, F.; Muhr, H.-J.; Niederberger, M.; Bieri, F.; Schnyder, B.; Nesper, R. *J. Am. Chem. Soc.* **1999**, *121*, 8324.

(13) Reinoso, J. M.; Muhr, H.-J.; Krumeich, F.; Bieri, F.; Nesper, R. *Helv. Chim. Acta* **2000**, *83*, 1724.

(14) Delmas, C.; Cognac-Auraadou, H.; Cocciantelli, J. M.; Ménétrier, M.; Doumerc, J. P. *Solid State Ionics* **1994**, *69*, 257.

(15) West, K.; Zachau-Christiansen, B.; Jacobsen, T.; Atlung, S. *J. Power Sources* **1985**, *14*, 235.

(16) Pistoia, G.; Pasquali, M.; Wang, G.; Li, L. *J. Electrochem. Soc.* **1990**, *137*, 2365.

have shown that electrodes made from  $\text{Na}^+$ -,  $\text{K}^+$ -, and  $\text{Ca}^{2+}$ - $\text{VO}_x$  nanotubes can be charged and discharged for at least 100 cycles, with maximum capacities of  $\sim 200 \text{ mA}\cdot\text{h/g}$ .<sup>3</sup> Ion-exchanged samples perform better than the as-synthesized material (containing dodecylamine). Surprisingly, all materials experience an increasing capacity within the first 20 cycles, and for some materials the increase can be over 100%.<sup>3</sup> Results presented later in this paper may give a possible explanation for this behavior.

Soft X-ray absorption spectroscopy (SXAS) and X-ray photoelectron spectroscopy (XPS) are applicable tools to investigate the electronic structure of both anode and cathode materials aimed at rechargeable Li batteries. Vanadium oxides have previously been subjected to detailed SXAS<sup>17–20</sup> and XPS<sup>18,21–23</sup> studies due to their interesting electronic and magnetic properties. SXAS probes the unoccupied electronic states and thus provides local chemical information about the sample. XPS probes core electrons ejected from the sample. Chemical shifts induced by changed electronic states give information about the chemical composition of the sample as well as on the oxidation state of a specific element. Element specificity allows investigation on one selected constituent of the cathode or anode. Hence, interference from other electrode components, which can cause problems in, for example, X-ray diffraction studies, are eliminated.

In this work, we have used SXAS and XPS to investigate the redox behavior of nanotubular vanadium oxide by monitoring the changes of the electronic states following the insertion of  $\text{Li}^+$  ions.  $\text{Na}^+$  ion-exchanged nanotubes ( $\text{Na-VO}_x$ ) have been chosen for this study, since they have shown good electrochemical properties.<sup>1</sup> Both of these methods are surface sensitive ( $< 50 \text{ \AA}$ ) and do not give any information about the bulk material. However, soft X-ray emission data, presented elsewhere,<sup>24</sup> give a better view of the electrode material closer to the current collector.

## Experimental Section

**Synthesis.** The  $\text{VO}_x$  nanotubes were prepared as described by Krumeich et al.<sup>10,12</sup> Vanadium(V) triisopropoxide,  $((\text{CH}_3)_2\text{CHO})_3\text{VO}$  (Aldrich), was used as a precursor and dodecylamine,  $\text{C}_{12}\text{H}_{25}\text{NH}_2$  (Aldrich, 99%), as a structure-directing molecule. The synthesis resulted in a black powder, consisting of  $\text{VO}_x$  nanorolls, which was washed in ethanol and dried under vacuum at  $80^\circ\text{C}$  for  $> 12 \text{ h}$ . The powder consisted largely of spherical conglomerates of nanotubes.

The ion exchange was performed as described by Krumeich et al.<sup>12</sup> using  $\text{NaCl}$  (puriss., Kebo). The product was washed and dried as above.

**Electrochemical Measurements.** Electrodes were prepared by extrusion of a slurry containing 80 wt %  $\text{Na-VO}_x$  nanotubes, 10 wt % carbon black (Shawinigan Black, Chevron), and 10 wt % ethylene-propylene-diene terpolymer (EPDM) binder onto an aluminum foil. Circular electrodes (20 mm in diameter) were dried under vacuum overnight inside an argon-filled glovebox ( $\text{O}_2/\text{H}_2\text{O} < 2 \text{ ppm}$ ) prior to use. The mass loading on the electrodes was  $\sim 1.5 \text{ mg/cm}^2$ .

Two-electrode cells were assembled in the glovebox, using  $\text{Na-VO}_x$  nanotubes as working electrode, a glass fiber cloth soaked in electrolyte as separator, and lithium metal as counter electrode. The electrolyte was 1 M lithium bis-(trifluoromethylsulfonyl)imide ( $\text{LiTFSI}$ , Rhodia) in ethylene carbonate (EC)/dimethyl carbonate (DMC) (both Selectipur, Merck), 2:1 by volume. The solvents were used as received, whereas the salt was dried under vacuum at  $120^\circ\text{C}$  for 24 h in the glovebox prior to use. The cell components were vacuum-sealed into polymer-coated aluminum pouches.

All cells were discharged and charged galvanostatically between 1.8 and 3.5 V (all potentials are given vs  $\text{Li/Li}^+$ ) using a Digatron MBT testing unit, with BTS-600 software. Initially, the cells were exposed to one discharge/charge cycle, applying 5 mA/g. After the first cycle was completed, the cells were slowly discharged to 3.0, 2.5, 2.0, and 1.8 V, respectively, using 1 mA/g current loading (corresponding to a discharge rate of 130 h). The electrodes were then equilibrated at the chosen potential for at least 30 days. The pouch cells were disassembled inside the glovebox, and the electrodes were washed in DMC to remove excess electrolyte and dried under vacuum at room temperature for 12 h.

Average oxidation states were calculated from the electrochemical data together with elemental information obtained from inductively coupled plasma (ICP) analysis. The electrochemically calculated values are based on the number of transferred electrons per vanadium atom at a given potential. Since the weights of the active material in the electrodes are known, we used this together with the weight percent of vanadium (from the ICP analysis) to calculate the number of moles of vanadium in the active material. By using the charge (in  $\text{A}\cdot\text{h}$ ) passed to a certain potential, we can estimate the number of electrons transferred per mole of vanadium. The initial oxidation state was approximately set according to results from the XPS measurements.

**Characterization.** Powder X-ray diffraction (XRD) was performed on a SIEMENS D5000 diffractometer ( $\text{Cu K}\alpha$  radiation,  $\lambda = 1.5418 \text{ \AA}$ ) between  $2^\circ$  and  $50^\circ$  in  $2\theta$ . The powders were evenly distributed on a zero-background Si plate.

The soft X-ray absorption measurements were performed at beam line I511 at the Swedish National Synchrotron Radiation Laboratory, MAX-II, Lund, Sweden. The base pressure in the experimental chamber was  $< 4 \times 10^{-9} \text{ mbar}$ . To avoid contact with air, the samples were premounted on sample holders in an argon-filled glovebox and carefully transported to the analysis chamber. A glovebag was fitted to the load-lock hatch of the vacuum introduction chamber, and the setup was purged with pure argon to ensure an inert atmosphere before the samples were transferred. All samples were transferred in one single operation. Absorption spectra were recorded measuring the total electron yield (TEY) from the sample as a function of incident photon energy. All spectra were normalized to the photocurrent from a clean gold mesh introduced into the beam. Reference samples, consisting of  $\text{V}_2\text{O}_5$ ,  $\text{V}_6\text{O}_{13}$ ,  $\text{VO}_2$ , and  $\text{V}_2\text{O}_3$  single crystals, were measured at the same beam line earlier.

XPS measurements were conducted on a PHI 5500 system using a monochromatized  $\text{Al K}\alpha$  anode as excitation source ( $h\nu = 1486.6 \text{ eV}$ ). The electrodes were carefully transported to the analysis chamber under inert atmosphere using a purpose-built device. The pressure in the chamber during analysis was  $< 4 \times 10^{-9} \text{ mbar}$ . Peak fitting was performed with XPSPEAK 4.1 software<sup>25</sup> using Voigt profiles together with a

(17) Schmitt, T.; Duda, L. C.; Augustsson, A.; Guo, J. H.; Nordgren, J.; Downes, J. E.; McGuinness, C.; Smith, K. E.; Dhalenne, G.; Revcolevshi, A.; Klemm, M.; Horn, S. *Surf. Rev. Lett.* **2002**, *9*, 1369.

(18) Passerini, S.; Ba Le, D.; Smyrl, W. H.; Berrettoni, M.; Tossici, R.; Marassi, R.; Giorgetti, M. *Solid State Ionics* **1997**, *104*, 195.

(19) Abbate, M.; Pen, H.; Czyzyk, M. T.; de Groot, F. M. F.; Fuggle, J. C.; Ma, Y. J.; Chen, C. T.; Sette, F.; Fujimori, A.; Ueda, Y.; Kosuge, K. *J. Electron Spectrosc. Relat. Phenom.* **1993**, *62*, 185.

(20) Meisel, A.; Hallmeier, K. H.; Szargan, R.; Müller, J.; Schneider, W. *Phys. Scr.* **1990**, *41*, 513.

(21) Demeter, M.; Neumann, M.; Reichelt, W. *Surf. Sci.* **2000**, *454–456*, 41.

(22) Mendialdua, J.; Cassanova, R.; Barbaux, Y. *J. Electron Spectrosc. Relat. Phenom.* **1995**, *71*, 249.

(23) Sawatzky, G. A.; Post, D. *Phys. Rev. B* **1979**, *20*, 1546.

(24) Augustsson, A.; Schmitt, T.; Duda, L. C.; Nordgren, J.; Nordlinder, S.; Edström, K.; Gustafsson, T.; Guo, J. H. Submitted to *J. Appl. Phys.* **2003**.

(25) Program written by Dr. Kwok, Chinese University of Hong Kong.

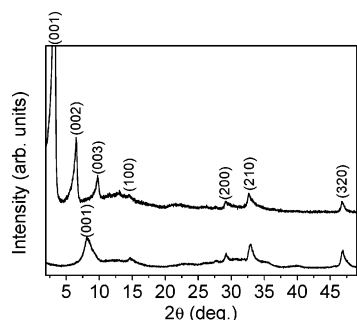


**Figure 1.** Powder diffractograms of the as-synthesized material containing dodecylamine (top) and the Na<sup>+</sup>-exchanged material (bottom).

Shirley background function. The same peak shape (75% Gaussian) and the same full width at half-maximum (fwhm = 1.5 eV) were applied for all V 2p<sub>3/2</sub> peak fits. The integrated areas (*A*) of the V 2p peaks were fitted with  $A(V\ 2p_{3/2}) = 0.5A(V\ 2p_{1/2})$ . The C 1s peak from carbon black in the composite electrodes was located at  $284.54 \pm 0.07$  eV. The displayed spectra and binding energies have not been subjected to energy correction.

Electrostatic charging effects, due to formation of insulating LiF, are observed in the spectra as a shift to higher binding energies for vanadium, oxygen, lithium, and fluorine as the electrodes are discharged. The effect is largest for Li 1s and F 1s (approximately +1.0 eV). V 2p and O 1s are both shifted approximately +0.50 eV relative to the binding energies in the pristine material. However, the difference in binding energy between O 1s and V(IV) 2p<sub>3/2</sub> is constant for the electrodes.

## Results and Discussion

**XRD.** Figure 1 displays the powder XRD pattern for the as-synthesized material, containing dodecylamine, and the Na<sup>+</sup> ion-exchanged material. The peaks at  $2\theta < 15^\circ$  are 00l reflections, typical for layered structures. The 001 peak corresponds to the distance between the VO<sub>x</sub> sheets. Removal of the amine in favor of the cation results in a decrease of the interlayer distance and thereby a shift in the 001 peak. For the as-synthesized and the Na-exchanged material, the interlayer distances are 27 and 9 Å, respectively. Peaks at  $2\theta > 15^\circ$  originate from the structure within the VO<sub>x</sub> layers. These reflections do not shift when the embedded guests changes. Therefore, it can be deduced that the intralayer structure is independent of the guest ion.

The diffractograms can be indexed on the basis of an approximate tetragonal unit cell with  $a \approx 6.1$  Å, which is in agreement with earlier results. It has been suggested that the structure within the VO<sub>x</sub> layers is similar to the double-layered vanadium oxide structure in BaV<sub>7</sub>O<sub>16</sub>·*n*H<sub>2</sub>O,<sup>26</sup> which has a tetragonal unit cell with  $a = 6.160$  Å.<sup>2,3,12</sup> On the basis of this assumption and a single-crystal XRD study of V<sub>7</sub>O<sub>16</sub> with embedded ethylene amine, Wörle et al.<sup>27</sup> recently determined the structure to be triclinic.

**Electrochemical Measurements.** The discharge profile for a Na-VO<sub>x</sub> electrode, shown in Figure 2 (inset), is continuous without plateaus. Included for reference is the long-term cycling behavior for a separate Na-VO<sub>x</sub> electrode cycled at a C/5 rate (one dis-

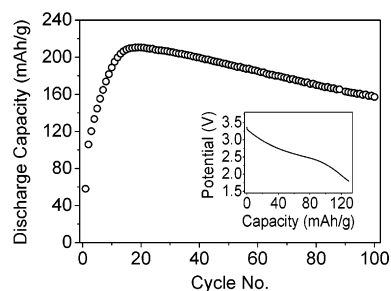


**Figure 2.** Discharge capacity as a function of cycle number for a Na-VO<sub>x</sub> electrode cycled with LiTFSI electrolyte at a C/5 rate (one discharge takes 5 h). The inset shows the discharge profile.

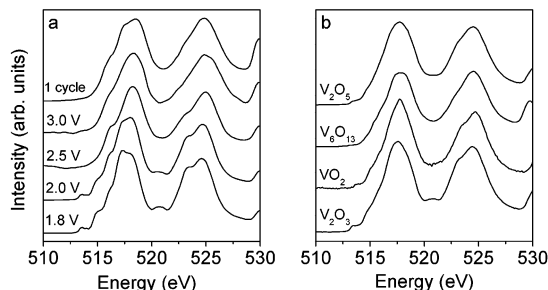


**Figure 3.** (a) V 2p SXA spectra of Na-VO<sub>x</sub> electrodes. The top spectrum is for an electrode cycled one time. (b) V 2p SXA spectra of reference materials.

charge takes 5 h). As discussed in the Introduction, a large increase in capacity can be seen over the first 20 cycles, but the reason for this behavior is not yet fully understood.

Discharging the electrochemical cell will lead to reduction of the cathode material. Originally, the VO<sub>x</sub> nanotubes are of mixed valence, with ~60% V(V) and ~40% V(IV) (the oxidation states are discussed further in the XPS section). Reducing all vanadium present in the VO<sub>x</sub> nanotubes one step [60% V(V) → V(IV) and 40% V(IV) → V(III)] gives a theoretical capacity of approximately 240 mA·h/g.<sup>3</sup> The maximum capacity for the Na-VO<sub>x</sub> electrode, shown in Figure 2, is 210 mA·h/g. Major contributions from any side reactions can be excluded since the Coulombic efficiency is >96% at all times.

**SXAS.** Figure 3a shows absorption spectra for the discharged electrodes and for an electrode cycled one time. Since the pristine material shows the exact same features as the electrode cycled one time, we have chosen to show only the latter. The spectra of four reference samples, V<sub>2</sub>O<sub>5</sub> (3d<sup>0</sup>), VO<sub>2</sub> (3d<sup>1</sup>), V<sub>2</sub>O<sub>3</sub> (3d<sup>2</sup>), and V<sub>6</sub>O<sub>13</sub> (d<sup>2/3</sup>), are displayed in Figure 3b. Transitions from V 2p core states to unoccupied 3d states give rise to the spin-orbit splitting in the SXA spectra: L<sub>3</sub> (2p<sub>3/2</sub> → 3d) at 515–520 eV and L<sub>2</sub> (2p<sub>1/2</sub> → 3d) at 522–527 eV.

Reduction from V(V) to V(IV) and V(III) increases the occupancy of electrons in the 3d states from d<sup>0</sup> (V(V)) to d<sup>2</sup> (V(III)), which will in turn enhance the screening of the core hole and thereby lead to a lower absorption energy. This effect can be clearly seen here, where the overall peak weight is shifted toward lower energies when Li<sup>+</sup> ions are inserted. A shoulder on the low-energy side of the L<sub>2</sub> peak (523 eV) increases in intensity, and the L<sub>3</sub> peak shifts toward lower energy. The electrodes discharged to 2.0 and 1.8 V show a small

(26) Wang, X.; Liu, L.; Bontchev, R.; Jacobson, A. J. *Chem. Commun.* **1998**, 1009.

(27) Wörle, M.; Krumeich, F.; Bieri, F.; Muhr, H. J.; Nesper, R. Z. *Anorg. Allg. Chem.* **2002**, 628, 2778.



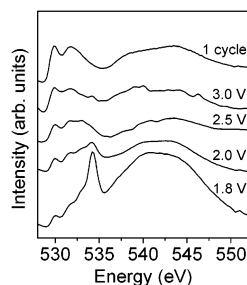


**Figure 4.** O 1s SXA spectra of Na-VO<sub>x</sub> electrodes. The top spectrum is for an electrode cycled one time.

peak at 520.7 eV, which appears to be the same characteristic peak found in the valley between L<sub>3</sub> and L<sub>2</sub> for V<sub>2</sub>O<sub>3</sub>. There are also some pre-edge structures in the energy region of 513.5–516 eV observed in both electrodes and the V<sub>2</sub>O<sub>3</sub> reference sample (Figure 3b and refs 19, 28, 29). The experimental findings suggest that the chemical surroundings of vanadium in the 2.0 and 1.8 V electrodes are very similar to that in V<sub>2</sub>O<sub>3</sub>, thus indicating the presence of V(III) in the material. The fact that the electrode subjected to one cycle does not show these features indicates a reversible reduction process. SXES measurements have been performed on the same electrodes, and the results suggest the same conclusions.<sup>24</sup> Since in that case, not electrons but photons are detected, the emission data probe the bulk structure of the material (up to 200 nm). Consequently, the existence of V(III) in the discharged electrodes is not only a surface effect.

The VO<sub>x</sub> nanotubes display considerable O 1s absorption at energies above 530 eV (Figure 4) due to the unoccupied O 2p bands which are strongly hybridized with V 3d and V 4sp bands. The oxygen spectra are divided in two distinct regions. Peaks at 530–537 eV are attributed to O 2p bands hybridized with V 3d bands, and the broad peak at 537–550 eV originates from hybridization with V 4sp bands. For vanadium oxides, the former region is generally split into two peaks, as can be seen for the material cycled one time in Figure 4. These peaks are found for all transition metal oxides in octahedral or similar symmetries and can be identified with t<sub>2g</sub> and e<sub>g</sub> bands separated by the ligand-field splitting. Details concerning assignments of different spectral absorption features can be found in, e.g., refs 19, 29–33. Due to weaker V 3d–O 2p hybridization for higher valencies, the relative intensity of the t<sub>2g</sub> and e<sub>g</sub> bands decrease as lithium is inserted into the material,<sup>19,30</sup> as can be seen in Figure 4.

After one cycle, the spectrum clearly shows two peaks (529.9 and 531.8 eV) in the O 2p–V 3d hybridization region. As lithium is inserted (reduction of vanadium), another feature at 534.3 eV starts to appear and increases in intensity. This peak is similar to that of

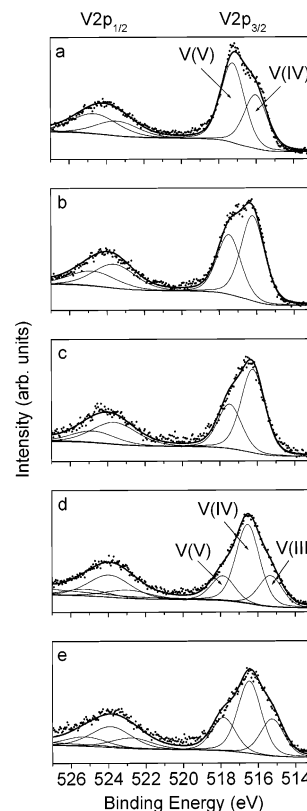


**Figure 5.** XPS V 2p spectra for the pristine electrode (a) and electrodes discharged to 3.0 (b), 2.5 (c), 2.0 (d), and 1.8 V (e). The fitted Voigt functions for V(V), V(IV), and V(III) are marked in the spectra to make the identification easier. The solid lines represent the individual peaks and the total fit. The experimental data are represented by dots.

surface carbonate.<sup>34</sup> Therefore, this peak is attributed to a surface layer consisting of decomposed electrolyte species, a so-called solid electrolyte interface (SEI) layer. Results from XPS measurements also point to the existence of an SEI layer on the electrode, as will be discussed later.

Mansour et al. recently studied the lithium insertion into V<sub>2</sub>O<sub>5</sub> aerogels by in situ K-edge X-ray absorption.<sup>35</sup> They conclude that the vanadium is first reduced from V(V) to V(IV), followed by further reduction of V(IV) to V(III) when more lithium ions are inserted. For the mixed-valence VO<sub>x</sub> nanotubes studied here, it is difficult to draw conclusions on the specific reduction behavior from absorption spectra alone. Therefore, XPS measurements were performed to get an estimate of the distribution of oxidation states for the different electrodes.

**XPS.** Figure 5 presents the V 2p XPS results for the pristine electrode (Figure 5a) and the discharged electrodes (Figure 5b–e). A typical two-peak structure can be seen in the spectra, originating from the spin–orbit splitting of V 2p<sub>3/2</sub> at 514–518 eV and V 2p<sub>1/2</sub> at 522–526 eV. When the electrodes are discharged, the shape of the V 2p peaks changes significantly. The peak weight is shifted toward lower binding energies, consistent with the absorption spectra.

To interpret the changing of peak shapes, the experimental spectra of the electrodes discharged to 3.0 and

(28) Pen, H. F.; Tjeng, L. H.; Pellegrin, E.; de Groot, F. M. F.; Sawatzky, G. A. *Phys. Rev. B* **1997**, *55*, 15500.

(29) deGroot, F. M. F.; Fuggle, J. C.; Thole, B. T.; Sawatzky, G. A. *Phys. Rev. B* **1990**, *42*, 5459.

(30) Zimmermann, R.; Claessen, R.; Reinert, F.; Sterner, P.; Hüfner, S. *J. Phys.: Condens. Matter* **1998**, *10*, 5697.

(31) Soriano, L.; Abbate, M.; Fuggle, J. C.; Jiménez, M. A.; Sanz, J. M.; Mythen, C.; Padmore, H. A. *Solid State Commun.* **1993**, *87*, 699.

(32) van der Laan, G.; Kirkman, I. W. *J. Phys.: Condens. Matter* **1992**, *44*, 4189.

(33) de Groot, F. M. F.; Grioni, M.; Fuggle, J. C. *Phys. Rev. B* **1989**, *40*, 5715.

(34) Madix, R. J.; Solomon, J. L. *Surf. Sci.* **1988**, *197*, L253.

(35) Mansour, A. N.; Smith, P. H.; Baker, W. M.; Balasubramanian, M.; McBreen, J. *Electrochim. Acta* **2002**, *47*, 3151.

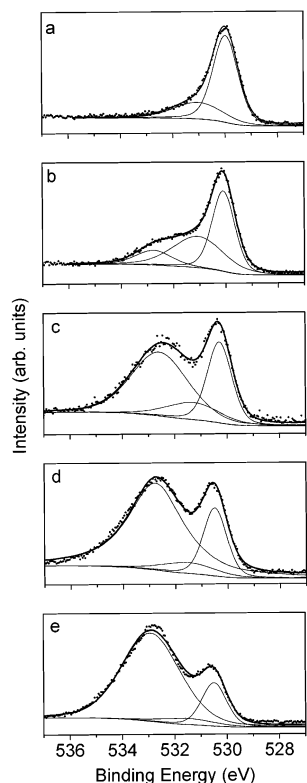


**Figure 6.** XPS O 1s spectra for the pristine electrode (a) and electrodes discharged to 3.0 V (b), 2.5 V (c), 2.0 V (d), and 1.8 V (e). The solid lines represent the individual peaks and the total fit. The experimental data are represented by dots.

**Table 1. XPS Binding Energies (in eV) for the Fitted Peaks<sup>a</sup>**

	V 2p <sub>3/2</sub>			O 1s	$\Delta$
	V(V)	V(IV)	V(III)		
pristine	517.3(0.60)	516.0(0.40)		530.0(1.01)	14.0
3.0 V	517.5(0.41)	516.2(0.59)		530.1(0.83)	13.9
2.5 V	517.5(0.34)	516.2(0.66)		530.3(0.83)	14.1
2.0 V	517.9(0.18)	516.5(0.59)	515.3(0.23)	530.5(0.69)	14.0
1.8 V	517.9(0.23)	516.5(0.51)	515.3(0.26)	530.5(0.64)	14.0

<sup>a</sup> Numbers in parentheses give the area of the individual peak divided by the total V 2p<sub>3/2</sub> area. The energy difference between V(IV) 2p<sub>3/2</sub> and O 1s (in eV) is displayed as  $\Delta$ .

2.5 V were deconvoluted with two Voigt functions, one representing V(V) at  $\sim 517.5$  eV and the other representing V(IV) at  $\sim 516.2$  eV (Figure 5a–c). For the electrodes discharged to 2.0 and 1.8 V (Figure 6d,e), a third peak had to be included, which indicates the presence of a new oxidation state, V(III), as seen earlier in the absorption spectra. The relation between the areas of the fitted peaks can then be seen as a measure of the different oxidation states of vanadium. Binding energies for the V 2p<sub>3/2</sub> peak and relative areas of the fitted peaks are displayed in Table 1. Originally, the material contains around 40% V(IV), which is consistent with earlier results from Krumeich et al.,<sup>12</sup> who estimated the V(IV) content of VO<sub>x</sub> tubes containing dodecylamine to be 45%, corresponding to a formal oxidation state of +4.55. The interlayer structure has been shown to consist of V<sub>7</sub>O<sub>16</sub> layers, which gives an average oxidation state of +4.57.<sup>27</sup> Since ion exchange does not significantly alter the VO<sub>x</sub> structure, the oxidation state should be the same for the Na–VO<sub>x</sub> material. When the electrodes are discharged, the relative amount of V(IV)

increases (Figure 5). Intuitively, all the V(V) should be reduced first, followed by the reduction of V(IV) to V(III), and this is also what Masour et al. reported for V<sub>2</sub>O<sub>5</sub> aerogels.<sup>35</sup> In contrast, we observe the coexistence of three oxidation states at lower potentials. Some of the vanadium (both V(V) and V(IV)) is probably inaccessible for reduction during the first cycles and do not initially participate in the electrochemical process. This may explain the increasing capacity over the first 10–20 cycles.

The oxidation states of vanadium estimated from XPS spectra and those derived from electrochemical measurements agree well. Pristine material contains approximately 40% V(IV), equivalent to an oxidation state of +4.60. At 3.0 V, the oxidation state estimated from XPS is +4.41. As only  $\sim 0.05$  mol of electrons have been transferred per mol of vanadium at this potential, the oxidation state after one complete cycle must be closer to +4.50 than +4.60. The former oxidation state has therefore been used as an approximate starting point to roughly estimate the vanadium valence in the cycled electrodes. At 2.5 V,  $\sim 0.15$  mol of electrons has been transferred per mole of vanadium, which gives an average oxidation state of +4.35 (based on the starting value of +4.50). At 1.8 V,  $\sim 0.53$  mol of electrons has been transferred, giving an oxidation state of +3.97. From XPS measurements, the oxidation states at the same potentials are estimated to +4.34 and +3.97, respectively, which is in good agreement.

Oxygen atoms bonded to vanadium atoms in the VO<sub>x</sub> structure give rise to a peak close to 530 eV in the O 1s XPS spectra (Figure 6). Binding energies for this peak are displayed in Table 1, together with the area relative to the total V 2p<sub>3/2</sub> peak area. The pristine electrode has a second peak at 531 eV, appearing as a shoulder, which originates from the binder and/or adsorbed water. As the electrode is discharged, a peak at 531–535 eV increases in intensity, from relatively small at 3.0 V to dominant at 1.8 V. A peak at this binding energy is commonly found in electrodes after electrochemical cycling and can be assigned to electrolyte decomposition products.<sup>36–39</sup> This peak has been fitted with one Voigt function, but more likely it consists of several contributions. The relatively small peak at 531–535 eV in the 3.0-V electrode indicates that the process is reversible and also possibly potential dependent. A possible dissolution of the SEI layer is dependent on the nature of the electrolyte used and the chosen potential range, as well as on the electrode material itself. Reversible formation of a polymeric-type coating around nanoparticles of CuO and CoO,<sup>40,41</sup> as well as other metal oxides,<sup>42</sup> has been found to occur at lower potentials ( $< 1$  V). It is possible that we see a similar dissolution process

(36) Eriksson, T.; Andersson, A. M.; Bishop, A. G.; Gejke, C.; Gustafsson, T.; Thomas, J. O. *J. Electrochem. Soc.* **2002**, *149*, A69.

(37) Eriksson, T.; Andersson, A. M.; Gejke, C.; Gustafsson, T.; Thomas, J. O. *Langmuir* **2002**, *18*, 3609.

(38) Bar-Tow, D.; Peled, E.; Burstein, L. *J. Electrochem. Soc.* **1999**, *146*, 824.

(39) Aurbach, D.; Weissman, I.; Schechter, A. *Langmuir* **1996**, *12*, 3991.

(40) Dollé, M.; Poizot, P.; Dupont, L.; Tarascon, J. M. *Electrochem. Solid State Lett.* **2002**, *5*, A18.

(41) Débart, A.; Dupont, L.; Poizot, P.; Leriche, J. B.; Tarascon, J. M. *J. Electrochem. Soc.* **2001**, *148*, A1266.

(42) Poizot, P.; Laurelle, S.; Grugeon, S.; Tarascon, J. M. *J. Electrochem. Soc.* **2002**, *149*, A1212.

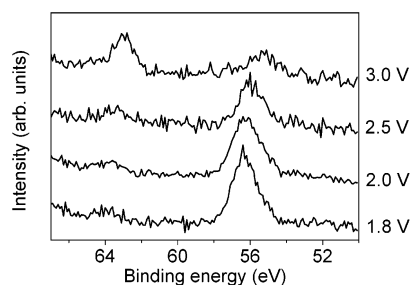


**Figure 7.** XPS Li 1s spectra of electrodes discharged to different potentials. The peak at 63.5 eV corresponds to Na 2s electrons.

occurring at higher potentials. What the exact constituents of this potentially reversible SEI layer around the  $\text{VO}_x$  nanotubes are, and how it is connected to the potential, however, are not yet known.

The Li 1s spectra (Figure 7) appear as a broad peak at 54–58 eV. The peak is most likely a superposition of several contributions, which can be attributed to, for example, LiF (55.7–56.5 eV),<sup>38,39,43,44</sup>  $\text{Li}_2\text{CO}_3$  or LiOH (55.2–55.5 eV),<sup>38,39,43</sup> and  $\text{Li}_2\text{O}$  (53.7 eV).<sup>38,39,43</sup> Lithium intercalated into the  $\text{VO}_x$  material would give rise to a peak close to 55 eV. This has been shown by Passerini et al., who found a broad Li 1s peak centered at 55 eV for chemically lithiated  $\text{V}_2\text{O}_5$  aerogels.<sup>18</sup> As the electrode is discharged, the intensity of the Li 1s peak at 54–58 eV increases. A part of the increase can probably be attributed to  $\text{Li}^+$  ions inside the  $\text{VO}_x$  nanotubes. However, the magnitude of this contribution is difficult to determine.

In the Li 1s spectra, a peak occurs at 62–64 eV (Figure 7), originating from Na 2s electrons (Na metal has a 2s binding energy of 63.5 eV<sup>45</sup>). This peak most likely originates from the  $\text{Na}^+$  ions embedded between

the  $\text{VO}_x$  layers. Interestingly, the intensity decreases with decreasing potential. Since we have evidence pointing to formation of a surface film, the Na 2s peak may be partly hidden in the background noise for the electrode materials at lower potential. Another possibility is removal of  $\text{Na}^+$  ions from the material as the electrode is discharged. However, more data are needed to confirm any of the two suggested scenarios.

The survey spectrum (not shown here) from the pristine electrode has a peak at 401 eV, corresponding to a nitrogen compound. This is most likely from dodecylamine left in the  $\text{VO}_x$  structure. The same peak, with approximately the same intensity, can be found in the cycled electrodes. A remainder of the amine after ion exchange has also been detected by Reinoso et al.<sup>13</sup>

## Conclusions

Both SXAS and XPS measurements of discharged Na– $\text{VO}_x$  nanotube electrodes point to a partial reduction to V(III) at potentials below 2.0 V. XPS measurements show a coexistence of V(V), V(IV), and V(III) at these potentials, indicating that some of the vanadium may be inaccessible to reduction. This is partly responsible for the increase in the capacity seen over the first 20 charge/discharge cycles.

**Acknowledgment.** This work has been supported by The Swedish Research Council (VR), The Nordic Energy Research Program (NERP) and The Göran Gustafssons Foundation (GGS). The authors thank Professor J. O. Thomas (Uppsala University) for his interest in this work. Dr. A. M. Andersson, M. Herstedt, and Dr. J. Lu (Uppsala University) are gratefully acknowledged for their help with the XPS measurements (A.M.A., M.H.) and the TEM characterization (J.L.). S.N. thanks Dr. T. A. Eriksson and Dr. A. Henningsson (Uppsala University) for helpful discussions.

CM031004G

(43) Kanamura, K.; Tamura, H.; Shiraishi, S.; Takehara, Z. *J. Electroanal. Chem.* **1995**, *394*, 49.

(44) Wagner, C. D.; Riggs, W. M.; Davis, L. E.; Moulder, J. F.; Muilenberg, G. E. *Handbook of X-ray Photoelectron Spectroscopy*; Physical Electronics Division, Perkin-Elmer Corp.: Eden Prairie, MN, 1979.

(45) Barrie, A.; Street, F. J. *J. Electron Spectrosc. Relat. Phenom.* **1975**, *7*, 1.